JOURNAL OF APPLIED PHYSICS **121**, 225103 (2017)

Superhard sp^2-sp^3 hybridized BC_2N: A 3D crystal with 1D and 2D alternate metallicity

Yufei Gao,[1] Yingju Wu,[1] Quan Huang,[2] Mengdong Ma,[1] Yilong Pan,[1] Mei Xiong,[1] Zihe Li,[1] Zhisheng Zhao,[1] Julong He,[1] and Dongli Yu[1,a)]
[1]*State Key Laboratory of Metastable Materials Science and Technology, Yanshan University, Qinhuangdao 066004, Hebei Province, China*
[2]*Center for High Pressure Science and Technology Advanced Research 1690 Cailun Rd., Bldg. #6, Pudong, Shanghai 201203, People's Republic of China*

(Received 24 February 2017; accepted 18 May 2017; published online 8 June 2017)

A novel sp^2-sp^3 hybridized orthorhombic BC_2N (o-BC_2N) structure (space group: *Pmm*2, No. 25) is investigated using first-principles calculations. O-BC_2N is constructed from multi-layers of C sandwiched between two layers of BN along the c axis; this structure contains sp^2- and sp^3-hybridized B-C, C-C, and C-N bonds. The structural stability of o-BC_2N is confirmed based on the calculation results for elastic constants and phonon dispersions. On the basis of the semi-empirical microscopic model, we speculate that the o-BC_2N compound is a potential superhard material with a Vickers hardness of 41.2 GPa. Calculated results for electronic band structures, density of states (DOS) and partial DOS (PDOS) show that the o-BC_2N crystal is metallic. The conducting electrons at the Fermi level are mostly from the 2p orbits of sp^2-hybridized B_4, N_1, and C_i (i = 2, 3, 4, 6, 7, 8) atoms, with slight contribution from the sp^3-hybridizd B_2 atoms. Furthermore, the calculated electron orbits of the o-BC_2N crystal demonstrate that the 2p orbits of the sp^2-hybridized atoms overlapped and formed π bonds. The electrons can conduct through the π bonds along the orientation parallel to the [100] and [010] directions in different layers, and the basal planes were formed by B_2-C_3-C_4 blocks, indicating that the o-BC_2N possesses the fascinating electronic property of linear-planar metallicity. *Published by AIP Publishing.* [http://dx.doi.org/10.1063/1.4984760]

I. INTRODUCTION

Ternary boron-carbon-nitrogen (B-C-N) compounds, which are anticipated to possess extreme hardness combined with adjustable band gap by changing their atomic composition and structure, have increasingly attracted attention due to their wide industrial application prospects.[1–12] Since the first synthesis of graphitic BC_2N (g-BC_2N) by Kouvetakis[5,13] and co-workers by using the chemical vapor deposition method, researchers have devoted efforts to obtain high-density BC_2N compounds experimentally[14–16] and theoretically.[9,17–21] Solozhenko *et al.*[16] have successfully synthesized c-BC_2N crystals under high temperature and high pressure conditions by using g-BC_2N as the raw material. The Vickers and Knoop hardness measurements suggested that the c-BC_2N phase was harder than the c-BN single crystal but still softer than diamond. A possible hetero-diamond β-BC_2N phase transformed from g-BC_2N was predicted by Tateyama *et al.*[19] The β-BC_2N phase displays a superior bulk modulus value of 438 GPa, which is close to that of diamond (464 GPa). Bond structure calculations showed that the β-BC_2N displays a band gap of 3.97 eV. In addition, many BC_2N phases have been obtained by replacing C atoms with B and N atoms in a diamond structure. Sun *et al.*[22] have investigated several c-BC_2N structures with a diamond-like unit cell by using the *ab initio* pseudopotential density functional method. Their results indicated that these c-BC_2N phases were direct band-gap semiconductors or semimetals with superior Vickers hardness values. Two novel types of o-BC_2N crystals were predicted by Mattesini[20] and co-workers. Their results showed that these o-BC_2N phases are possibly harder than c-BN, and their band gaps are 2.04 and 1.69 eV, respectively. The commonly proposed diamond-like BC_2N phases are either insulators or semiconductors due to electron localization in sp^3 hybridized atoms and the isoelectronic properties of $(BN)_2$ and C units.

Nevertheless, crystals with sp^2-sp^3 hybrid characteristics, such as T-B_7N_7[23] and 3D-(n, 0) carbons,[24] exhibit metallicity because of the intensified electron delocalization of sp^2 configuration with a short distance between the adjacent atomic layers. A novel orthorhombic B_3N_5 (o-B_3N_5) structure (space group $C222_1$) was recently reported by Li *et al.*[25] The o-B_3N_5 contains one type of B atoms and two types of N (N1 and N2) atoms. B and N1 atoms are four-coordinated, and each N2 atom is sp^2 hybridized with two B atoms and one N2 atom. This sp^2-sp^3 hybridized structure possesses surprising properties, such as a narrow band gap of 0.775 eV, a high energy density of approximately 3.44 kJ/g, and an increased Vickers hardness of 44 GPa.

This paper reports on a novel sp^2-sp^3 mixed hybridization o-BC_2N structure, which is produced by replacing a part of B and N atoms with C atoms in the o-B_3N_5 unit cell. The o-BC_2N is a sandwich-like structure constructed from C layers alternately stacked with BN layers along the c axis. sp^2- and sp^3-hybridized B, C, and N atoms coexist in this structure. Using the first-principles density-functional method, we investigated the ground-state properties of the o-BC_2N structure. The calculated results show that the o-BC_2N structure displays

a)Email: ydl@ysu.edu.cn. Tel: + 86 13933565368.

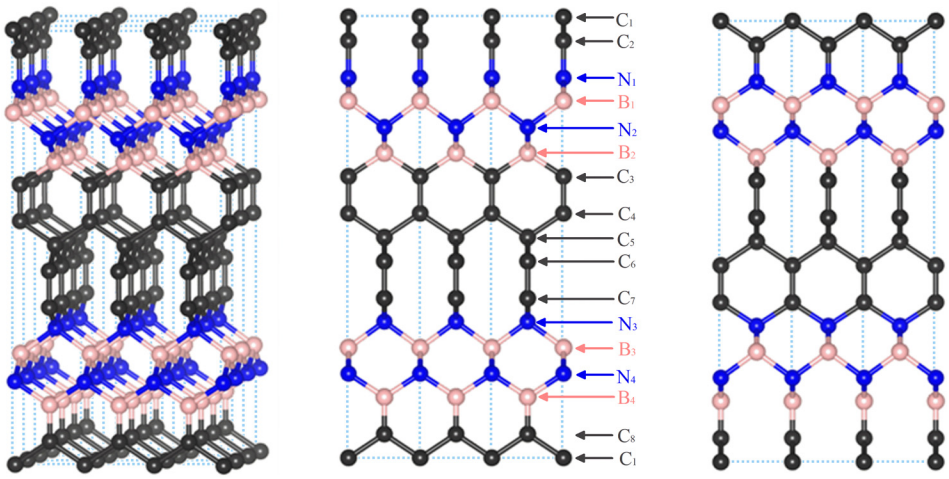

FIG. 1. The relaxed crystal structure (a) and views along the [010] (b) and [100] (c) directions of the o-BC_2N. The boron, carbon, and nitrogen atoms are described as pink, black, and blue colors, respectively.

the distinctive electronic property of linear-planar metallicity. The Vickers hardness of the o-BC_2N crystal is approximately 41.2 GPa, indicating that o-BC_2N is a potential superhard metallic material.

II. CALCULATION METHODS

First-principles calculations were performed using the pseudopotential density functional method[26] implemented in the CASTEP code.[27] The Perdew–Berke–Ernzerhof form of the generalized gradient approximation (GGA-PBE) was used to treat the exchange-correlation function.[28] To ensure an accurate determination of electronic properties, calculations are repeated using the hybrid Heyd–Scuseria–Ernzerhof functional (HSE06).[29,30] The ultrasoft pseudopotential[31] was expanded by the plane-wave basis set with a cutoff energy of 770 eV. Elastic constants, bulk modulus, and shear modulus can be calculated directly by using the CASTEP code. Structural relaxation was performed using the Broyden–Fletcher–Goldfarb–Shanno methods.[32] The phonon modes of the equilibrium crystal structure were calculated through finite displacement theory[33] using a k-point space ($2\pi \times 0.015\,\text{Å}^{-1}$) corresponding to the fine quality level. The coordinates of the high symmetry points in reciprocal space are $Y(-0.5,0,0)$, $G(0,0,0)$, $Z(0,0,0.5)$, $T(-0.5,0,0.5)$, $R(-0.5,0.5,0.5)$, $U(0,0.5,0.5)$, $X(0,0.5,0)$, and $S(-0.5,0.5,0)$. The supercell volume is 16 times that of the cell in the phonon calculations. The energy band structures and PDOS calculations used the k points which were selected with a $9 \times 9 \times 2$ mesh in the Brillouin zone. The Vickers hardness of the o-BC_2N crystal is estimated using the microscopic theoretical hardness model.[34–37]

TABLE I. Atomic Wyckoff positions of the o-BC_2N structure.

Atom	Wyckoff positions	Atom	Wyckoff positions
B_1	1a (0, 0, 0.807)	C_1	1a (0, 0, -0.002)
B_2	1d (0.5, 0.5, 0.691)	C_2	1b (0, 0.5, 0.945)
B_3	1b (0, 0.5, 0.251)	C_3	1b (0, 0.5, 0.637)
B_4	1c (0.5, 0, 0.141)	C_4	1b (0, 0.5, 0.551)
N_1	1b (0, 0.5, 0.862)	C_5	1d (0.5, 0.5, 0.498)
N_2	1c (0.5, 0, 0.752)	C_6	1c (0.5, 0, 0.446)
N_3	1d (0.5, 0.5, 0.310)	C_7	1c (0.5, 0, 0.362)
N_4	1a (0, 0, 0.195)	C_8	1c (0.5, 0, 0.048)

III. RESULTS AND DISCUSSIONS

Figure 1 shows the o-BC_2N crystal structure after structural relaxation, and Table I presents the atomic Wyckoff positions of o-BC_2N. The o-BC_2N structure exhibits a sandwich-like layer structure constructed from C layers separated from BN layers along the c axis. A number of sp^2- and sp^3-hybridized B, C, and N atoms formed a mixed hybridization o-BC_2N structure. Table II shows the calculated lattice parameters, total energies E_t, bulk moduli B, and shear moduli G of o-BC_2N, o-B_3N_5, diamond, and c-BN structures. For comparison, the experimental values for diamond and c-BN are also shown in Table II. The errors in lattice parameters, bulk moduli, and shear moduli between the calculated and experimental values for diamond and c-BN are very small, indicating that the calculated results are satisfactory. The calculated lattice constants a, b, and c of o-BC_2N are 2.627, 2.544, and 15.817 Å, respectively. The bulk modulus B of o-BC_2N is 310 GPa, which is equal to that of o-B_3N_5. The shear modulus G of o-BC_2N is 435 GPa lower than that of diamond but higher than that of o-B_3N_5 and c-BN.

The formation energy (E_f) of o-BC_2N was calculated according to the formula $E_f = E_{BC_2N} - (E_{c\text{-}BN} + 2E_C)$, where E_{BC_2N}, $E_{c\text{-BN}}$, and E_c represent the energy of BC_2N, c-BN, and

TABLE II. Lattice parameters, formation energy (E_f), bulk modulus B and shear modulus G of the o-BC_2N, o-B_3N_5, diamond and c-BN structures after structural optimization.

Structure	o-BC_2N	o-B_3N_5	Diamond	c-BN
Symmetry	$Pmm2$	$C222_1$	F-43m	F-43m
a (Å)	2.627	3.642 (3.638[a])	3.568 (3.567[b])	3.627 (3.615 [b])
b (Å)	2.554	3.639 (3.636[a])		
c (Å)	15.817	15.883 (15.834[a])		
E_f (eV/atom)	0.53	0.42		
B (GPa)	310	309 (328[a])	424 (443[c])	369 (400[c])
G (GPa)	435	266 (289[a])	522 (535[c])	380 (409[c])

[a]Reference 25.
[b]Reference 14.
[c]Reference 39.

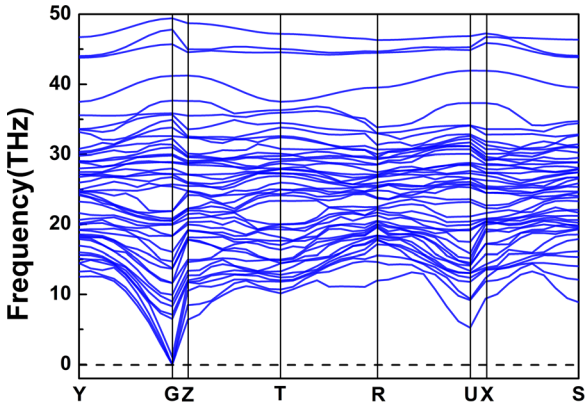

FIG. 2. The phonon dispersion curves for o-BC_2N.

diamond formula unit, respectively. The positive formation energy indicates that the o-BC_2N phase is metastable and tends to dissociate into c-BN and diamond. To check the structural stability of the o-BC_2N phase, its elastic stiffness constants (GPa) are calculated as follows: $C_{11} = 720.7$, $C_{22} = 683.2$, $C_{33} = 943.9$, $C_{44} = 73.1$, $C_{55} = 139.2$, $C_{66} = 126.5$, $C_{12} = 27.5$, $C_{13} = 104.6$, and $C_{23} = 117.0$. For the orthorhombic structures, the generalized elastic stability criteria is $C_{ii} > 0$ (i = 1, 2…6), $[C_{11} + C_{22} + C_{33} + 2\,(C_{12} + C_{13} + C_{23})] > 0$, $(C_{11} + C_{22} - 2\,C_{12}) > 0$, $(C_{11} + C_{33} - 2\,C_{13}) > 0$, and $(C_{22} + C_{33} - 2\,C_{23}) > 0$.[38] The elastic constants of the o-BC_2N structure satisfy the mechanical stability criteria, suggestive of its mechanical stability. The calculated phonon dispersion curves (Fig. 2) demonstrate that the o-BC_2N structure is dynamically stable because of the absence of imaginary frequencies in the entire Brillouin zone.

To explore the electronic properties of the o-BC_2N structure, the band structures are calculated by standard DFT and hybrid functional HSE06 methods. The GGA/PBE calculated results show that there are four occupied bands (marked 31, 32, 33, and 34) crossing the Fermi level in Fig. 3(a), which indicates that the o-BC_2N crystal may possess metallicity. It is generally known that the standard DFT calculations would underestimate the band gap. Hence, we completed the verification calculation for the band structure of o-BC_2N using the screened hybrid functional HSE06 method shown in Fig. 3(b). The result shows that the DFT calculation underestimated the band gap for 0.154 eV. Comparing both the band structures, we found no significant changes for the position of energy bands from 31 to 34, although the band gap value was underestimated by DFT calculation.

The calculated total density of states (DOS) and the partial DOS (PDOS) of B_i ($i = 1, 2, 4$), N_j ($j = 1 \sim 3$) and C_k ($k = 1 \sim 3$, $6 \sim 8$) atoms in the o-BC_2N structure are shown in Fig. 4. The PDOS of B_3, N_4, C_4, and C_5 atoms are similar to those of B_1, N_3, C_6, and C_1, respectively. The conducting electrons at the Fermi level are mostly from the $2p$ electrons of B_4, N_1, and C_i (i = 2, 3, 4, 6, 7, 8) atoms with sp^2-hybridized states. The sp^3-hybridizd B_2 atoms slightly contributed to the electron state at the Fermi level. The contribution of B_1, B_3, C_1, C_5, N_2, N_3, and N_4 is very small and can be negligible.

Figure 5 shows the electron orbits of four occupied bands crossing the Fermi level [31 to 34 in Fig. 3(a)] in the o-BC_2N structure. The projection of the electron orbital along the b axis of the o-BC_2N structure is shown in Fig. 5(a). We divided the projection into four regions marked

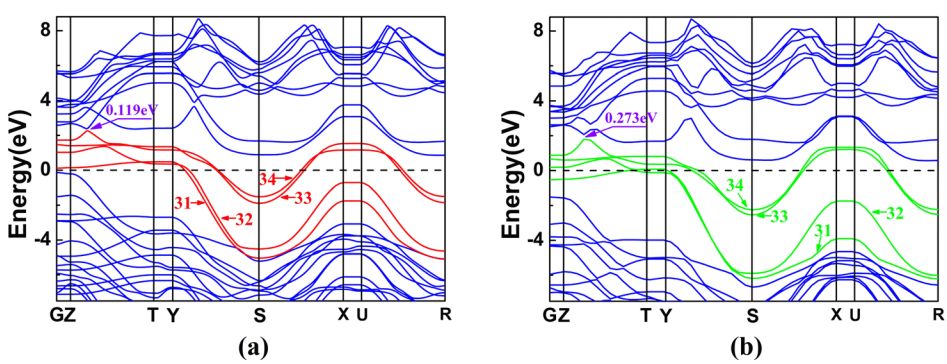

FIG. 3. The electronic structures of o-BC_2N: GGA/PBE (a) and HSE06 (b). The Fermi level is indicated by the horizontal dashed line.

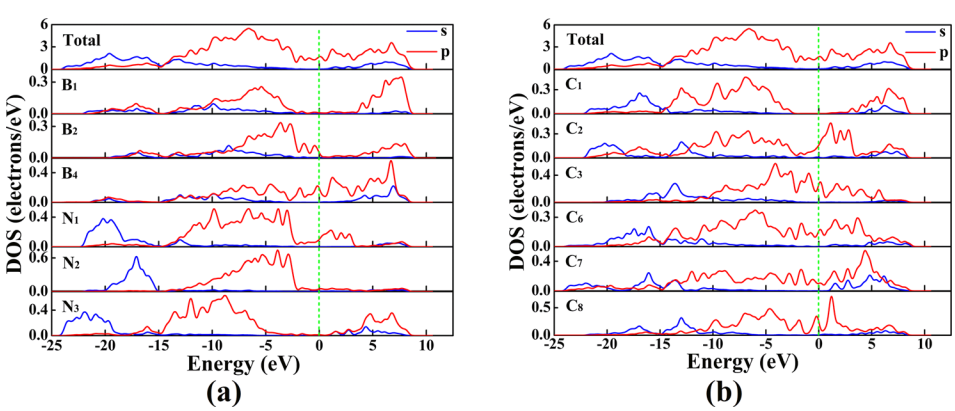

FIG. 4. Total density of states, s (blue line) and p (red line) partial density of states of the o-BC_2N structure. The Fermi level is indicated by the green dashed line.

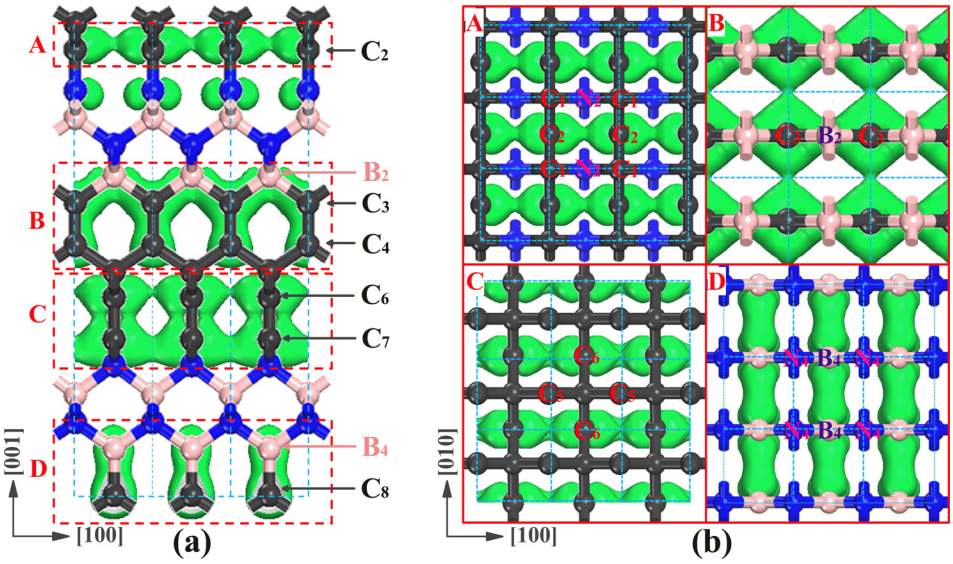

FIG. 5. Calculated electron orbits of the o-BC_2N structure. Panel (a) shows the projection of an electron orbital viewing along the [010] direction and panel (b) shows four projections of the electron orbitals viewing along the [001] direction which corresponds to the local fragments [marked red rectangle squares in panel 5(a)].

with A, B, C, and D. In the A, B, and C regions, the electron orbits are overlapped along the [100] crystal orientation and envelop the C_2 atom chain, the B_2-C_3-C_4 triatomic layer and the C_6-C_7 diatomic layer, respectively. In the D region, the electron orbit only covers the B_4-C_8 diatomic units. It is worth noting that the electron orbits crossing the Femi level in the regions of A, B, C, and D are disconnected in the [001] crystal orientation of the o-BC_2N structure, which implies that the conduction electrons are blocked in the c axis of the o-BC_2N crystal. The electron orbits in A, B, C, and D areas are projected along the c axis of the crystal structure and presented in Fig. 5(b), respectively. Based on the projections along the b and c axes of the o-BC_2N structure, we can confirm that the electron orbits in the A, C, and D regions formed one dimensional chain distributions (1D), respectively, around C_2, C_6-C_7 ([100] direction) and B_4-C_8 ([010] direction) atoms. In the B region, the electron orbits formed two dimensional distributions (2D) rounding B_2-C_3 atoms along the [100] direction and C_3-C_4 atoms following the [010] direction.

Combined with the analyses of the energy band structures and electron orbits, we consider that the electrons in the o-BC_2N structure can conduct through the linked electron orbits near the Femi level along the orientation parallel to the [100] and [010] directions in different layers, which indicate that the new o-BC_2N crystal may possess a fascinating electronic property with 1D and 2D alternate metallicity.

Based on our semi-empirical microscopic hardness theoretical model,[32–35] the Vickers hardness of o-BC_2N can be calculated by the formula as follows: $H_v(GPa) = AN_e^{2/3}d^{-2.5}e^{-1.191f_i-32.2f_m^{0.55}}$. In the formula, A is a content 350, N_e is the electron density, d is the bond length of each x–y chemical bond, f_i is the Phillips ionicity of the chemical bond, which can be calculated by $f_i = [1 - \exp(-|P_c - P|/P)]^{0.735}$, and f_m is a factor of metallicity written as $f_m = 0.026D_F/n_e$, where D_F is the electron density of states at the Fermi level, and n_e is the total number of the valence electrons in a unit cell.[35] Bond parameters of the o-BC_2N crystal obtained from first-principles calculations are listed in Table III. Here we obtained the pure covalent population P_c by calculation of the overlap population of the C-C bonds in the supercell with 128 carbon atoms stacking on the basis of the o-BC_2N structure. The calculated Vickers hardness of the o-BC_2N is 41.2 GPa, which indicates that it is a potential superhard material. Combining with the novel electronic property of o-BC_2N, this unique crystallographic characteristic of o-BC_2N is expected to possess some potential applications in electronic devices, such as metal-solid dielectric-vacuum junction, metal-insulator "multiple quantum well" devices, and photonic devices. Meanwhile, the o-BC_2N crystal may be manufactured into a special anvil with conductivity used in high pressure installations.

IV. CONCLUSIONS

A distinctive sp^2-sp^3 hybridized o-BC_2N structure is predicted. The o-BC_2N is constructed from C layers sandwiched between BN layers and contains sp^2- and sp^3-hybridized B, C, and N atoms. Calculations of elastic constants and phonon frequencies have confirmed the structural stability of o-BC_2N. The electronic band structures, DOS, and PDOS

TABLE III. Chemical bond parameters and Vickers hardness of o-BC_2N.

Bond type	d	Pop	P_c	N_e	f_i	f_m (10^{-3})	H_v
C1-C2	1.521	0.85	0.87	0.629	0.063	0.627	41.2
C2-C3	1.359	1.43	1.47	1.009	0.071	1.864	
C3-C4	1.558	0.85	0.87	0.586	0.063	1.161	
C4-C5	1.517	0.86	0.87	0.635	0.037	0.611	
C5-C6	1.338	1.45	1.47	1.056	0.042	0.864	
C7-C8	1.544	0.87	0.87	0.602	0	0.928	
C2-N1	1.304	1.21	1.47	1.284	0.298	0.777	
C6-N3	1.519	0.69	0.90	0.700	0.374	0.388	
B2-C2	1.570	0.92	0.90	0.511	0.059	1.153	
B4-C7	1.465	1.30	1.47	0.704	0.213	1.636	
B1-N1	1.545	0.72	0.90	0.497	0.329	0.324	
B1-N2	1.577	0.77	0.80	0.483	0.090	0.204	
B2-N2	1.597	0.65	0.80	0.466	0.313	0.220	
B3-N3	1.611	0.66	0.80	0.454	0.296	0.150	
B3-N4	1.551	0.72	0.80	0.509	0.191	0.145	
B4-N4	1.567	0.72	0.80	0.555	0.191	0.775	

show that the o-BC_2N crystal exhibits a metallic character, and the conducting electrons at the Fermi level are mostly from the $2p$ orbits of sp^2-bonded atoms, with small contributions from the sp^3-bonded B_2 atom. Studies on electron orbits demonstrate that the electrons can transmit along the parallel forming around the C_2, C_6, and C_7 atoms along the [100] direction, and around the B_4, and C_8 atoms along the [010] direction, and on the basal planes consisting of the B_2-C_3-C_4 atoms in the o-BC_2N crystal. Consequently, the o-BC_2N possesses a fascinating electronic property characterized by 1D and 2D metallicity, which is distinct from the conventional BC_2N phases, namely, semimetals, semiconductors, or insulators. The theoretical Vickers hardness of o-BC_2N is approximately 41.2 GPa, which is suggestive of its superhard property. This study of the unique metallic BC_2N structure offers a new method to explore the ternary B-C-N compounds possessing diverse electrical properties, rendering immense application prospects for these compounds in electronic devices.

ACKNOWLEDGMENTS

This work was supported by the National Science Foundation of China (Grant Nos. 51672238, 51421091, 51332005, and 51572235).

[1]X. G. Luo and J. L. He, Chin. Phys. Lett. **29**(3), 036104 (2012).
[2]M. Kawaguchi, S. Kuroda, and Y. Muramatsu, J. Phys. Chem. Solids **69**, 1171 (2008).
[3]J. L. He, L. C. Guo, E. Wu, X. G. Luo, and Y. J. Tian, J. Phys. Condens. Matter **16**, 8131 (2004).
[4]X. G. Luo, X. J. Guo, Z. Y. Liu, J. L. He, D. L. Yu, Y. J. Tian, and H. T. Wang, J. Appl. Phys. **101**, 83505 (2007).
[5]J. Kouvetakis, T. Sasaki, C. Shen, R. Hagiwara, M. Lerner, K. M. Krishnan, and N. Bartlett, Synth. Met. **34**, 1 (1989).
[6]X. G. Luo, Z. Y. Liu, J. H. He, B. Xu, D. L. Yu, H. T. Wang, and Y. J. Tian, J. Appl. Phys. **105**, 43509 (2009).
[7]M. Kawaguchi, Y. Wakukawa, and T. Kawano, Synth. Met. **125**, 259 (2001).
[8]X. G. Luo, X. F. Zhou, Z. Y. Liu, J. L. He, B. Xu, D. Yu, H. T. Wang, and Y. J. Tian, J. Phys. Chem. C **112**, 9516 (2008).
[9]Q. Li, M. Wang, A. R. Oganov, T. Cui, Y. M. Ma, and G. T. Zou, J. Appl. Phys. **105**, 53514 (2009).
[10]X. G. Luo, L. Y. Li, W. H. Wang, and Y. J. Tian, J. Appl. Phys. **109**, 023516 (2011).
[11]V. L. Solozhenko, High Presssure Res. **22**, 519 (2002).
[12]K. Raidongia, K. Hembram, U. V. Waghmare, M. Eswaramoorthy, and C. N. R. Rao, Z. Anorg. Allg. Chem. **636**, 30 (2010).
[13]R. B. Kaner, J. Kouvetakis, C. E. Warble, M. L. Sattler, and N. Bartlett, Mat. Res. Bull. **22**, 399 (1987).
[14]E. Knittle, R. B. Kaner, R. Jeanloz, and M. L. Cohen, Phys. Rev. B **51**, 12149 (1995).
[15]Y. Zhao, D. W. He, L. L. Daemen, T. D. Shen, R. B. Schwarz, Y. Zhu, D. L. Bish, J. Huang, J. Zhang, G. Shen, J. Qian, and T. W. Zerda, J. Mater. Res. **17**, 3139 (2002).
[16]V. L. Solozhenkoa, D. Andrault, G. Fiquet, M. Mezouar, and D. C. Rubie, Appl. Phys. Lett. **78**, 1385 (2001).
[17]X. G. Luo, X. J. Guo, B. Xu, Q. H. Wu, Q. K. Hu, Z. Y. Liu, J. L. He, D. L. Yu, and Y. J. Tian, Phys. Rev. B **76**, 094103 (2007).
[18]X. G. Luo, X. J. Guo, Z. Y. Liu, J. L. He, D. L. Yu, B. Xu, and Y. J. Tian, Phys. Rev. B **76**, 092107 (2007).
[19]Y. Tateyama, T. Ogitsu, K. Kusakabe, S. Tsuneyuki, and S. Itoh, Phys. Rev. B **55**, R10161 (1997).
[20]M. Mattesini and S. F. Matar, Int. J. Inorg. Mater. **3**, 943 (2001).
[21]Y. Zhang, H. Sun, and C. F. Chen, Phys. Rev. Lett. **93**, 195504 (2004).
[22]H. Sun, S. H. Jhi, D. Roundy, M. L. Cohen, and S. G. Louie, Phys. Rev. B **64**, 094108 (2001).
[23]S. H. Zhang, Q. Wang, Y. Kawazoe, and P. Jena, J. Am. Chem. Soc. **135**, 18216 (2013).
[24]Z. S. Zhao, B. Xu, L. M. Wang, X. F. Zhou, J. L. He, Z. Y. Liu, H. T. Wang, and Y. J. Tian, ACS Nano **5**, 7226 (2011).
[25]Y. W. Li, J. Hao, H. Y. Liu, S. Y. Lu, and S. T. John, Phys. Rev. Lett. **115**, 105502 (2015).
[26]M. Segall, P. J. Lindan, M. a. Probert, C. Pickard, P. Hasnip, S. Clark, and M. Payne, J. Phys. Condens. Matter **14**, 2717 (2002).
[27]Y. Wang, J. Lv, L. Zhu, and Y. Ma, Comput. Phys. Commun. **183**, 2063 (2012).
[28]J. P. Perdew, K. Burke, and M. Ernzerhof, Phys. Rev. Lett. **77**, 3865 (1996).
[29]J. Heyd, G. E. Scuseria, and M. Ernzerhof, J. Chem. Phys. **118**, 8207 (2003).
[30]J. Heyd, G. E. Scuseria, and M. Ernzerhof, J. Chem. Phys. **124**, 219906 (2006).
[31]D. Vanderbilt, Phys. Rev. B **41**, 7892 (1990).
[32]T. H. Fischer and J. Almlof, J. Phys. Chem. **96**, 9768 (1992).
[33]S. J. Clark, M. D. Segall, C. J. Pickard, P. J. Hasnip, M. I. Probert, K. Refson, and M. C. Payne, Z. Kristallogr. Cryst. Mater. **220**, 567 (2005).
[34]X. J. Guo, L. Li, Z. Y. Liu, D. L. Yu, J. L. He, R. P. Liu, B. Xu, Y. J. Tian, and H. T. Wang, J. Appl. Phys. **104**, 023503 (2008).
[35]F. M. Gao, J. L. He, E. D. Wu, S. M. Liu, D. L. Yu, D. C. Li, S. Y. Zhang, and Y. J. Tian, Phys. Rev. Lett. **91**, 015502 (2003).
[36]J. L. He, E. D. Wu, H. T. Wang, R. P. Liu, and Y. J. Tian, Phys. Rev. Lett. **94**, 015504 (2005).
[37]M. D. Ma, B. C. Yang, Z. H. Li, M. Hu, Q. Q. Wang, L. Cui, D. L. Yu, and J. L. He, Phys. Chem. Chem. Phys. **17**, 9748 (2015).
[38]J. P. Watt, J. Appl. Phys. **50**, 6290 (1979).
[39]D. M. Teter, MRS Bull. **23**, 22 (1998).